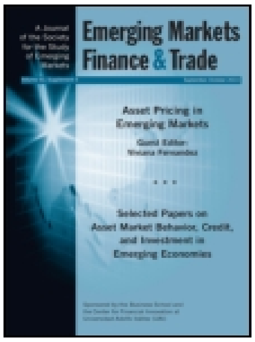

Emerging Markets Finance and Trade

ISSN: 1540-496X (Print) 1558-0938 (Online) Journal homepage: http://www.tandfonline.com/loi/mree20

Credit Risk in Interbank Networks

Vanessa Hoffmann De Quadros, Juan Carlos González-Avella & José Roberto Iglesias

To cite this article: Vanessa Hoffmann De Quadros, Juan Carlos González-Avella & José Roberto Iglesias (2015) Credit Risk in Interbank Networks, Emerging Markets Finance and Trade, 51:sup6, S27-S41, DOI: 10.1080/1540496X.2015.1080554

To link to this article: http://dx.doi.org/10.1080/1540496X.2015.1080554

Published online: 09 Oct 2015.

Emerging Markets Finance & Trade, 51:S27–S41, 2015

ISSN: 1540-496X print/1558-0938 online
DOI: 10.1080/1540496X.2015.1080554

Credit Risk in Interbank Networks

Vanessa Hoffmann De Quadros[1], Juan Carlos González-Avella[1], and José Roberto Iglesias[1,2]

[1]*Instituto de Física, Universidade Federal do Rio Grande do Sul, Porto Alegre, RS, Brazil;* [2]*Programa de Mestrado em Economia, Universidade do Vale do Rio dos Sinos, São Leopoldo, RS, Brazil*

ABSTRACT: One of the most striking characteristics of modern financial systems is their complex interdependence, comprising a network of bilateral exposures in the interbank market, in which institutions with surplus liquidity can lend to those with a liquidity shortage. Empirical studies reveal that some interbank networks have features of scale-free networks. We explore the characteristics of financial contagion in networks whose distribution of links approaches a power law, using a model that defines banks' balance sheets from information on network connectivity. By varying the parameters for the creation of the network, several interbank networks are built, in which the concentration of debt and credit comes from the distribution of links. The results suggest that networks that are more connected and have a high concentration of credit are more resilient to contagion than other types of networks analyzed.

KEY WORDS: complex networks, contagion, financial crashes, interbank exposure, power laws, systemic risk

Introduction

The 2007–08 financial crisis highlighted, once again, the high degree of interdependence in financial systems. A combination of excessive borrowing, risky investments, lack of transparency, and high interdependence led the financial system to its worst meltdown since the Great Depression. An increasing interest in financial contagion, partially motivated by the crisis, gave rise to several works in this field in the past few years (see, among others, Craig and von Peter 2014; Montagna and Lux 2014).

The interdependence of financial systems is manifested in multiple ways. Financial institutions are connected through mutual exposure created in the interbank market, through which institutions with surplus liquidity can lend to those with a liquidity shortage. Equally important, financial institutions are indirectly connected by having exposure in the same assets and by sharing the same depositors.

With respect to the direct connection from having mutual exposure, the structure of interdependence can be easily illustrated in a visual representation of a network, in which the nodes of the network are financial institutions, while the links are the exposure between nodes. The direction of the link indicates the cash flow at the time of debt repayment (from debtor to creditor) as well as the direction of the effect or financial loss if borrowers default on their repayment.

Theoretical works (Allen and Gale 2000; Freixas, Parigi, and Rochet 2000) have shown that the possibility of contagion via mutual exposure depends on the precise structure of the interbank market. In recent studies, different models have been used to generate artificial interbank networks in order to identify whether a given network is more or less prone to contagion.

Nier et al. (2007) simulate contagion from the initial failure of a bank in an Erdös-Rényi random network, finding a negative nonlinear relationship between contagion and bank connectivity. An increase in the amount of interbank exposure initially has no effect on contagion since the losses are absorbed by each affected node. However, as the number of connections rises, contagion increases

Address correspondence to Vanessa Hoffmann De Quadros, Instituto de Física, Universidade Federal do Rio Grande do Sul, Caixa Postal 15051, 90501-970 Porto Alegre RS, Brazil. E-mail: vhquadros@gmail.com

Color versions of one or more of the figures in the article can be found online at www.tandfonline.com/MREE.

to the point that a further increase in connectivity causes contagion to decline. The nonmonotonic relationship between connectivity and contagion found by the authors reflects two phenomena. The addition of new links adds new channels through which contagion can occur. However, additional links also represent the distribution of losses among a larger number of nodes, diluting the effect of the failure and mitigating the effects of the contagion.

Studying a specific case of power-law network, Cont and Moussa (2010) find results similar to those of Nier et al. (2007) regarding the relation between connectivity, the level of capitalization, and contagion.

Battiston et al. (2012) simulate contagion in a regular network and find a nonlinear relationship between connectivity and contagion, but with the opposite effect: Initially, the increase in the number of connections decreases network contagion, while later additions cause contagion to increase.

Ladley (2013) evaluates the relation between connectivity and contagion in a partial equilibrium model of heterogeneous banks interacting in the interbank market. The author shows that, under small systemic shocks, higher connectivity increases resilience against contagion; larger shocks have the opposite effect.

The differences in the results indicate that the possibility and extent of contagion depend considerably on the structure of the network and the specific assumptions of each model.

Empirical studies reveal that some interbank networks have features of scale-free networks. This means that the distribution of connections among banks follows a power law, $p(k) \sim k^{-X}$ (Boss et al. 2004; Cont et al. 2010; Inaoka et al. 2004; Soramäki et al. 2007).[1] Drawing on this stylized fact, Montagna and Lux (2014) simulate networks whose link distribution follows power laws in order to evaluate the relevance of some known quantities (like the size of the banks) for contagion measures.[2]

In general terms, some of the most significant features reported in the literature can be summarized as follows:

- Networks have a low density of links; that is, they are far from complete;
- They exhibit asymmetrical in-degree and out-degree distributions;
- They exhibit approximate power-law distributions for in- and out-degree distributions whose exponent varies around 2–3.

A characteristic reported by Cont et al. (2010) in a study of the Brazilian network is also worth noting: There is a positive association between the size of the exposure (assets) and the number of debtors (in-degree) of an institution and a positive association between the size of liabilities and the number of creditors (out-degree) of an institution. More (less) connected financial institutions have a larger (smaller) exposure.

The goal of this article is to identify, through simulations of networks whose distributions approach power laws, how scale-free networks behave with regard to financial contagion via mutual exposure and which characteristics make a given network more or less prone to propagate crises. Our particular interest is in evaluating the role of the exponents that characterize a scale-free network because these exponents determine the concentration of debt (out-degree) and credit (in-degree) in the financial network. We construct networks whose connectivity distribution approaches a power law using the algorithm introduced by Bollobás et al. (2003). Using a simplified model that determines the banks' balance sheets from information on network connectivity, we divide each balance sheet into bank assets and bank liabilities and nonbank assets and nonbank liabilities.

By varying the parameters for the creation of the network, several interbank networks are built, in which the concentration of debt and credit comes from the distribution of links. Three main types of interbank network are analyzed for their resilience to contagion: (1) those where the concentration of debt is greater than the concentration of credit, (2) those where the concentration of credit is greater than the concentration of debt, and (3) those with similar concentrations of debt and credit. For all the networks that we have generated, the financial contagion starts with the failure of a single node, which affects neighboring nodes by defaulting on its obligations in the interbank lending market. Thus, this work focuses on the problem of credit risk, disregarding other equally important sources of contagion, as the risk of adverse shocks spreads to several institutions at the same time.

Generating Scale-Free Networks

In their study on scale-free networks, Barabasi and Albert (1999) propose a preferential attachment mechanism to explain the emergence of the power-law degree distribution in nondirected graphs. The algorithm proposed by Bollobás et al. (2003) is a generalization for directed networks of the model developed by Barabasi and Albert (1999). The network is formed using a preferential attachment that depends on the distribution of in-degree, k_{in}, and out-degree, k_{out}. This algorithm has the advantage of producing different exponents for in and out degrees, which are necessary for reproducing the characteristics of real networks. The following describes the steps for generating the network according to Bollobás et al. (2003).

Let α, β, γ, δ_{in}, and δ_{out} be nonnegative real numbers such that $\alpha + \beta + \gamma = 1$. Let G_0 be any initial network, and let t_0 be the number of links of G_0.[3] At each step t, starting with $t = t_0 + 1$, we add a new link to the network, so that in step t the network has t links and a random number of nodes, $n(t)$. At each step, the addition of the new link may or may not be accompanied by adding a new node, according to the following method (Bollobás et al. 2003):

1. At probability α, we create a new node v with a link from v to an existing node, u, selected with probability

$$p(u = u_i) = \frac{k_{in}(u_i) + \delta_{in}}{t + n(t)\delta_{in}}. \tag{1}$$

2. At probability β, we select an existing node v with probability

$$p(v = v_i) = \frac{k_{out}(v_i) + \delta_{out}}{t + n(t)\delta_{out}} \tag{2}$$

and add a link from v to an existing node u, chosen with probability

$$p(u = u_i) = \frac{k_{in}(u_i) + \delta_{in}}{t + n(t)\delta_{in}}. \tag{3}$$

3. At probability γ, we add a new node u with a link from an existing node v to u, where v is selected with probability

$$p(v = v_i) = \frac{k_{out}(v_i) + \delta_{out}}{t + n(t)\delta_{out}}, \tag{4}$$

where $k_{in}(u_i)$ is the in-degree of node u_i and $k_{out}(v_i)$ is the out-degree of node v_i. Because probability β refers to the addition of a link without the creation of a node, increasing the value of β implies increasing the average network connectivity. In turn, parameters α and γ are related to the addition of new nodes while increasing the connectivity of existing nodes.

Bollobás et al. (2003) show that when the number of nodes goes to infinity and connectivity grows, one obtains

$$p(k_{in}) \sim C_{IN} k_{in}^{-X_{IN}} \tag{5}$$

$$p(k_{out}) \sim C_{OUT} k_{out}^{-X_{OUT}}, \tag{6}$$

where:

$$X_{IN} = 1 + \frac{1 + \delta_{in}(\alpha + \gamma)}{\alpha + \beta} \tag{7}$$

$$X_{OUT} = 1 + \frac{1 + \delta_{out}(\alpha + \gamma)}{\beta + \gamma} \tag{8}$$

The limit $N \rightarrow \infty$ obviously cannot be achieved, but the result is valid when the number of nodes grows and we take the more connected ones; that is, power laws for k_{in} and k_{out} will emerge in the tail of the distribution of large networks.

We want to compare networks with different values for X_{IN} and X_{OUT} (featuring different concentrations of k_{in} and k_{out}) while keeping other characteristics, such as average connectivity and total concentration of links distribution, similar. We are particularly interested in networks with values of X_{IN} and X_{OUT} around 2–3, in accordance with estimated empirical values (e.g., Boss et al. 2004; Cont et al. 2010; Soramäki et al. 2007). We restrict the degrees of freedom of the model, imposing the following constraints on the parameters:[4]

$$\alpha + \gamma = 0.75 \text{ and } \delta_{in} + \delta_{out} = 4 \tag{9}$$

We consider δ_{in} and δ_{out} with ratios 1:3 or 3:1 in order to accentuate the asymmetry of the network. In addition to these constraints, we will cover the spaces of parameters $\alpha \times \gamma$ and $\delta_{out} \times \delta_{in}$ by sweeping the following radial lines:

$$\alpha = \frac{\delta_{out}}{\delta_{in}}\gamma \rightarrow \alpha = \frac{4 - \delta_{in}}{\delta_{in}}\gamma \tag{10}$$

The intersection points of Equation (10) with Equation (9) give us the set $(\alpha, \gamma, \delta_{in}, \delta_{out})$, which in turn define pairs (X_{IN}, X_{OUT}) as shown in Figure 1.

Using Equations (9) and (10) we restate parameters α, β, γ, and δ_{out} as functions of δ_{in}, and replacing such expressions in the equations for X_{IN} and X_{OUT}, respectively, we obtain the two parametric equations:

$$X_{IN} = 1 + \frac{16 + 12\delta_{in}}{16 - 3\delta_{in}} \text{ and } X_{OUT} = 1 + \frac{68 - 9\delta_{in}}{4 + 3_{\delta in}}, \tag{11}$$

from which we finally have

$$X_{OUT} = \frac{X_{IN} + 15}{X_{IN} - 1}. \tag{12}$$

The networks constructed using Equation (12) are therefore generated through variation of a single degree of freedom, with similar average connectivity and link concentration (limited by Equation (9)), differing in the value of pairs (X_{IN}, X_{OUT}).[5]

For our studies of contagion, we selected three points on the curve in Figure 1 (Equation (12)), representing three distinct networks, denominated as GD_0, S_0, and GC_0. The GD_0 network is more concentrated on the debtor side: With a higher concentration of debt than credit, it is generated so that

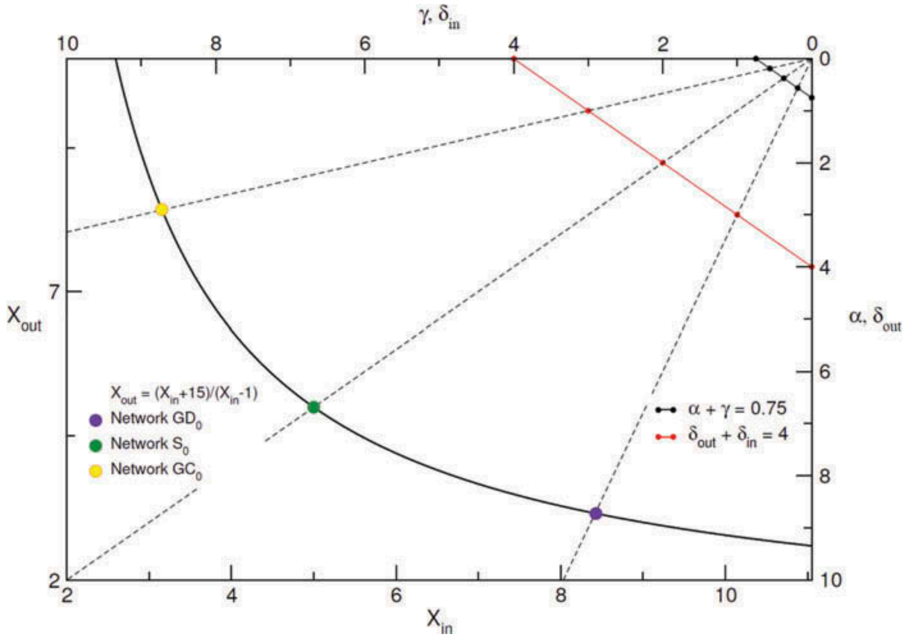

Figure 1. Parameter space and space of exponents: Spaces $\alpha \times \gamma$ and $\delta_{out} \times \delta_{in}$ are represented with origin in the upper-right corner and the space of exponents $X_{IN} \times X_{OUT}$ with origin at the bottom left.

Table 1. Limit values of the exponents X_{IN} and X_{OUT}, average connectivity, and Gini index for three selected networks

	X_{IN}	X_{OUT}	$< k >$	G	G_{in}	G_{out}
GD_0 network	8.4286	3.1538	2.646 (±0.039)	0.457 (±0.006)	0.418 (±0.013)	0.746 (±0.009)
S_0 network	5.0000	5.0000	2.663 (±0.041)	0.429 (±0.006)	0.578 (±0.015)	0.576 (±0.012)
GC_0 network	3.1538	8.4286	2.652 (±0.028)	0.456 (±0.008)	0.748 (±0.011)	0.410 (±0.008)

the largest banks in the network are major debtors in the system. The GC_0 network has a higher concentration of credit: The biggest banks are major creditors in the network. The S_0 network corresponds to the symmetric case, in which the concentrations of debt and credit are similar. The limit values (X_{IN}, X_{OUT}) for these networks are shown in Table 1.

Table 1 shows the limit values of the exponents X_{IN} and X_{OUT}, the values of the average connectivity for the generated networks, $< k >$, the Gini coefficient of the distribution of links, G, the Gini coefficient of the distribution of in-links (in-degree distribution), G_{in}, and the Gini coefficient of the distribution of out-links (out-degree distribution). The values in the table are average values over twenty simulations for networks with 1,000 nodes.

The choice of such values takes into account that we simulate small networks of 1,000 nodes (in accordance with real financial networks; e.g., Boss et al. 2004; Mistrulli 2011; Soramäki et al. 2007), for which the estimated exponents are below the limit values. Indeed, generating networks of 1,000 nodes with the selected parameters, we obtain exponents between 2.2 and 3.2. The estimation of the exponents of the power law of each distribution is performed using the maximum likelihood estimator for discrete power laws, according to Clauset et al. (2009).

To complete the information about an interbank network, it is necessary to assign weights to the links because the weights represent the magnitude of exposure among banks. The sum of in-degree weights of a bank, i, represents its applications in other institutions in the financial system (loans to other banks), a variable that we define as *bank assets, BA_i*. The sum of out-degree weights represents the total obligations of i to other financial institutions (loans from other banks), which we call *bank liabilities, BL_i*. If there is a link from bank j to bank i, we define the exposure of bank i to j by w_{ji}, such that

$$BA_i = \sum_{j \in \{k_{in}^i\}} w_{ji}, \tag{13}$$

where $\{k_{in}{}^i\}$ is the set of banks with obligations to bank i. Similarly, if there is a link from bank i to bank j, we define the obligation of bank i to bank j by w_{ij}, such that

$$BL_i = \sum_{j \in \{k_{out}^i\}} w_{ij}, \tag{14}$$

where $\{k_{out}{}^i\}$ is the set of banks to which bank i has obligations to pay.

In a study on the Brazilian interbank network, Cont et al. (2010) highlight the nonlinear positive relationship between link weights and connectivity of nodes in line with the widespread notion that the size of balance sheets and the connectivity of banks are positively related (Arinaminpathy et al. 2012). Drawing on this assumption, we define the following equation for the weight of a link from i to j:

$$w_{ij} = \frac{k_{out}^i \cdot k_{in}^j}{k_{out}^{\max} \cdot k_{in}^{\max}} \tag{15}$$

In Equation (15), $k_{in}{}^{max}$ and $k_{out}{}^{max}$ denote the maximum values of k_{in} and k_{out} found in the network.

Having established values for bank assets and bank liabilities, BA_i and BL_i, we define the other elements of the balance sheet: nonbank assets, NBA_i (all applications except interbank ones), nonbank liabilities, NBL_i (funding from outside the system), and equity, E_i.

For each bank, i, the balance sheet obeys the identity

$$BA_i + NBA_i = BL_i + NBL_i + E_i. \tag{16}$$

Reflecting the minimum capital regulations of the Basel accords, we set the equity of each bank as a proportion of its assets:

$$E_i = \lambda_i(BA_i + NBA_i), \tag{17}$$

where λ_i represents the capital–asset ratio.

For the simulations in this work, we use three values for a capital–asset ratio: undercapitalization, with $\lambda = 0.01$, and values $\lambda = 0.05$ and $\lambda = 0.1$, consistent with the empirical values observed (IMF 2013). For each bank, the capital–asset ratio is extracted from a normal distribution $\lambda_i \sim N(\lambda, \sigma)$ subject to the constraint $\lambda_i > \lambda$; that is, σ is a stochastic positive deviation from the minimum λ, characterizing the heterogeneity of banks with regard to capitalization. The simulations are performed using $\sigma = 0.01$.

To represent the ratio of nonbank assets to total assets, we introduce the following relation that defines nonbank assets for each bank, i, as

$$NBA_i = \xi(BA_i + BL_i). \tag{18}$$

Defined in this way, nonbank assets are a function of bank connectivity (via BA_i and BL_i), consistent with the assumption that balance sheet size is related to connectivity. Let us use ξ as a calibration factor to control the ratio of NBA_i to total assets.

Equations (16), (17), and (18) form a system of equations by which the value of NBL_i can be determined:

$$NBL_i = (1 - \lambda_i)(1 + \xi)BA_i + [(1 - \lambda_i)\xi - 1]BL_i \tag{19}$$

For the simulations in this work, we set $\xi = 2$ in order to obtain balance sheets in which nonbank assets and nonbank liabilities represent on average more than 50 percent of total assets and liabilities.

The banks' size, measured as the magnitude of their total assets ($NBA_i + BA_i$), presents a distribution with characteristics similar to that of the distribution of links but with estimated exponents ranging between 1.2 and 1.5, thereby having a higher concentration. In fact, the Gini coefficient for total asset concentration (Gini for the distribution $NBA_i + BA_i$) is 0.83 for the GC_0 network, 0.80 for the GD_0 network, and 0.78 for the S_0 network.[6]

From the method described in this section, we are able to represent the balance sheet of each bank by using only information from the network and the parameters λ and ξ. In the following section, we will describe the cascade of failures following the initial default of one bank of the network.

Contagion in Interbank Networks: Default Cascade and Default Effect

In this section, we present the methodology used to evaluate the propagation of losses in the interbank network. We simulate the insolvency of a single bank exposed to an external shock represented by the total loss of value of its nonbank assets. Each bank is tested independently and the effect of its default on the system evaluated.

In a hypothetical scenario, a bank, i, becomes insolvent, being unable to completely fulfill its obligations. If at time t, bank j realizes that its counterparty i is unable to repay its interbank liability w_{ij} in full, then bank j must reevaluate its application in bank i, from w_{ij} to w'_{ij}: $(w'_{ij} - w_{ij}) < 0$. This process adversely affects the capital of j, since variation $(w'_{ij} - w_{ij})$ is incorporated as a loss. It happens that the smaller value, w'_{ij}, the defaulting bank i can effectively afford, depends on the financial conditions of other banks, banks for which i had granted loans. Any further failure reduces the value of assets, increasing the losses of banks that have already defaulted.

Eisenberg and Noe (2001) study the problem of calculating the values w'_{ij} that banks would be able to pay at the time of settlement of its multilateral obligations. Given the array of mutual exposures, W, the problem is to determine the vector of payments, $p = (p_1, p_2, \ldots, p_n)$, *where*

$$p_i = \sum_{j=1}^{n} w'_{ij} \tag{20}$$

The authors show that under mild regularity conditions, there is a unique payment vector that settle the system, and they develop an iterative algorithm to solve the problem. In the context of our work, where we have a single node initially insolvent, the algorithm can be described as follows:

- Compute the losses to all banks resulting from the failure of bank i assuming that all other banks are able to repay their liabilities. Stop if no other bank fails, otherwise
- Let j denote the bank or group of banks whose losses exceed their equity. Compute the losses to all banks resulting from the failure of banks i and j. Repeat step 2 until no further bank fails.

The algorithm described allows us to calculate two important measures for assessing the effect of a bank failure: the *Default Impact* and the *Default Cascade*. For a bank, i, the *Default Impact*, DI_i, refers to the reduction in total assets of the financial system as a result of losses incurred via contagion, as a proportion of total initial assets. If we denote the total assets of the system at the initial time as A_0 and at the final time (after the external shock) as A_t, the *Default Impact* is given by the following:[7]

$$DI_i = \frac{A_0 - A_t - NBA_i}{A_0} \tag{21}$$

The measure *Default Cascade,* DC_i, refers to the number of insolvent banks due to the failure of bank i as a proportion of the total number of banks in the network. Both the *Default Impact* and the *Default Cascade* of a bank reveal how the network would be affected by its failure, taking into account only the direct effects of loss propagation through interbank exposures.

Results

We present the results obtained from contagion simulations for networks produced according to the prescription presented in the section "Generating Scale-Free Networks" of the present article. We consider three types of networks as previously defined: the GD_0 network, which has a higher concentration of debtors than creditors; the GC_0 network, which has a higher concentration of creditors; and the S_0 network, which has equal concentrations of creditors and debtors.

Default Impact and Default Cascade

For each set of parameters that defines a network category (GD_0, S_0, and GC_0), we performed twenty simulations, so that the analysis is based on twenty realizations of networks of type GD_0 networks, twenty realizations of S_0 networks, and twenty realizations of GC_0 networks. For each generated network and for each bank, i, the *Default Impact,* DI_i, and *Default Cascade,* DC_i, were calculated. The results presented in this section are for networks with 1,000 nodes, with capital level $\lambda = 0.05$.

Figure 2 shows the ranking of banks for the three networks, in decreasing order of DI_i. The values are average values for each ranking position; for example, for each network type the greater *Default Impact* (first-ranking position) is the average of greater impacts for twenty simulations. Equivalently, the subsequent positions of the ranking are average values.

The difference between the three types of networks is more pronounced in the first-ranking positions, although these positions show greater dispersion around the mean value.

The area under the ranking curve, which corresponds to the sum of individual impacts, should be considered as a measure of the network systemic risk. We then have for each network an aggregate measure, DI, given by

$$DI = \sum_{i=1}^{n} DI_i. \tag{22}$$

The measure DI corresponds to a measure of central tendency: In fact, if DI is divided by N (number of nodes), we have the average value for individual default impact. Ordering the three networks by the aggregate index, DI, we have the GD_0 network with a greater impact (DI = 0.48), followed by S_0 (DI = 0.46), and finally the GC_0 network (DI = 0.43) (see Figure 2). That means that a higher concentration of debt links corresponds to a greater impact.

However, if the three networks are evaluated according to their principal banks (first-ranking banks in the ranking), the GD_0 network remains in the first position of impact, but the other two switch positions: banks in the GC_0 network with a higher DI_i have a greater effect on the system than the big banks in the S_0 network. This fact can be explained by differences in the asset concentrations of the three networks GD_0, GC_0, and S_0. It happens that banks with large balance sheets have a stronger impact on the system, and although we have constructed the networks such that they have similar concentrations of connectivity, interbank exposures as defined by the model accentuate asset concentrations, which also increases the differences between them. The GC_0 network, which has the highest Gini coefficient, has a large bank, whose total assets are 122

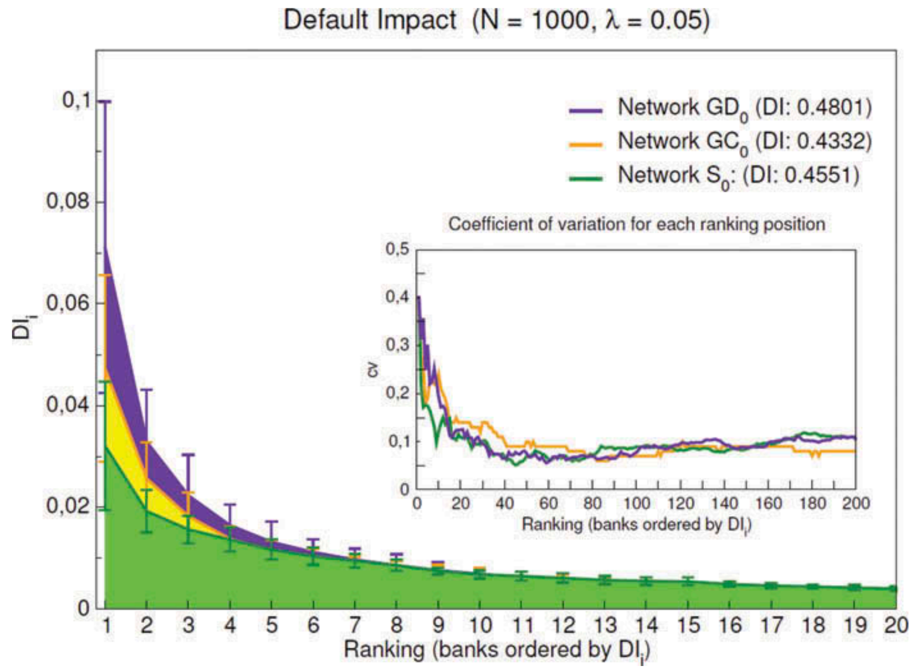

Figure 2. Ranking of banks in decreasing order of DI_i.

Notes: The figure shows the values for the twenty banks causing a major impact. Recall that, for each bank, i, the *Default Impact, DI_i*, refers to the losses suffered by the system via contagion (from the default of i) as a proportion of total assets in the network. The inset graph presents the values of the coefficient of variation ($cv = \sigma/\mu$) at each ranking position for the 200 banks with a greater impact.

times greater than the average assets in the network, while the largest bank in the symmetric S_0 network has total assets 55 times larger than average.

Comparison is more straightforward when the networks are evaluated by the *Default Cascade* of their nodes because in this case the difference is more pronounced. For the *Default Cascade*, we also define the area under the ranking curve as an aggregate measure:

$$DC = \sum_{i=1}^{n} DC_i \tag{23}$$

Here the ordering of the networks is clear. First, the GD_0 network has greater potential to generate contagion in case of the default of its nodes ($DC = 0.99$). Second, we have the symmetric S_0 network ($DC = 0.79$), and finally the GC_0 network ($DC = 0.49$). The size of the balance sheet has less influence on the *Default Cascade* than over the *Default Impact*, and the effect of concentrations of debt and credit links becomes more apparent. In fact, as expected, the *Default Cascade* increases with the increased concentration of debts. The bank that leads to a higher cascade in the GD_0 network reaches about 6 percent of the nodes in the network, compared with GC_0 network, where it reaches less than 1 percent, although these banks have similar sizes.

Effect of Connectivity and Link Concentration

Previous studies that simulate contagion in different network topologies address the question of the influence of connectivity on the propagation of losses. Conclusions differ, depending strongly on the structure of the networks used in each work.

Table 2. Parameter values used in the construction of networks of type 0, 1, 2, 3, and 4

	α	β	γ	δ_{in}	δ_{out}
GC_0	0.5625	0.2500	0.1875	1.00	3.00
S_0	0.3750	0.2500	0.3750	2.00	2.00
GD_0	0.1875	0.2500	0.5625	3.00	1.00
GC_1	0.1875	0.7500	0.0625	1.00	3.00
S_1	0.1250	0.7500	0.1250	2.00	2.00
GD_1	0.0625	0.7500	0.1875	3.00	1.00
GC_2	0.1875	0.7500	0.0625	25.00	75.00
S_2	0.1250	0.7500	0.1250	50.00	50.00
GD_2	0.0625	0.7500	0.1875	75.00	25.00
GC_3	0.5625	0.2500	0.1875	1.00	3.00
S_3	0.3750	0.2500	0.3750	2.00	2.00
GD_3	0.1875	0.2500	0.5625	3.00	1.00
GC_4	0.5625	0.2500	0.1875	10.00	30.00
S_4	0.3750	0.2500	0.3750	20.00	20.00
GD_4	0.1875	0.2500	0.5625	30.00	10.00

If we simply increase network connectivity through the addition of new random links, the distribution of connectivity becomes less concentrated, which also affects network performance in the propagation of losses. We would like to propose separating these two effects: the effect of connectivity variation and changes in concentration. Here the term "concentration" refers to the distribution of links, in the sense that a more concentrated network is one in which a few nodes have many links (hubs), while the majority of nodes have just a few. A less concentrated network has a more egalitarian distribution of links.

In an attempt to understand how these two features affect financial contagion, we have tested new types of networks that are variants of the three networks previously evaluated, with different levels of connectivity and concentration. Thus, in addition to the original type, which we have named type 0 and consists of GD_0, S_0, and GC_0, we have implemented four new types, each one detailed in the following sections. The type 1 networks have greater connectivity and are more concentrated than the original. Type 2 networks have greater connectivity than type 0 and similar concentration to type 0. Type 3 networks have greater connectivity than type 0 but are less concentrated. Finally, type 4 networks have the same connectivity as the original type, but with less concentration. Table 2 shows the parameters used in the construction of type 0, 1, 2, 3, and 4 networks.

Greater Connectivity and Greater Link Concentration

In this case, we have the GD_1, S_1, and GC_1, networks constructed such that they have greater connectivity and are more concentrated than the original ones. This is accomplished by increasing β from 0.25 to 0.75. We maintain the ratio 1:3 between α and γ and the same values of δ_{in} and δ_{out}. As the probability β refers to the addition of a new link without the creation of a new node, increasing β implies increasing the average network connectivity. As the connection mechanism is preferential attachment, an increase in β also increases the concentration of links. Table 3 shows the aggregate measures, *DI* and *DC*, as well as the average connectivity, the Gini coefficient for link concentration (G), the Gini coefficient for the distribution of credit links (G_{in}), and the Gini coefficient for the distribution of debt links (G_{out}).

The concentration of links has different effects depending on the symmetry of the network. As we move from the GC_0 network to the GC_1 network, we see a decrease in the contagion effect in response to the increased number of connections and higher concentration of credits (concentration

Table 3. Aggregate measures, *DI* and *DC*, < *k* >, *G*, G_{in} and G_{out}, for network types 0 and 1

	DI	*DC*	< *k* >	*G*	G_{in}	G_{out}
GC_0	0.433 (±0.001)	0.494 (±0.023)	2.652 (±0.028)	0.456 (±0.008)	0.748 (±0.011)	0.410 (±0.008)
S_0	0.455 (±0.004)	0.792 (±0.024)	2.663 (±0.041)	0.429 (±0.006)	0.578 (±0.015)	0.576 (±0.012)
GD_0	0.480 (±0.004)	0.988 (±0.015)	2.646 (±0.039)	0.457 (±0.006)	0.418 (±0.013)	0.746 (±0.009)
GC_1	0.426 (±0.001)	0.331 (±0.028)	7.406 (±0.166)	0.630 (±0.008)	0.805 (±0.010)	0.561 (±0.010)
S_1	0.429 (±0.001)	0.735 (±0.025)	7.484 (±0.227)	0.612 (±0.007)	0.669 (±0.009)	0.671 (±0.008)
GD_1	0.437 (±0.002)	1.113 (±0.027)	7.425 (±0.165)	0.630 (±0.008)	0.560 (±0.010)	0.805 (±0.007)

of in-links). The aggregate *Default Impact, DI*, does not suffer large variations, varying from 0.43 in GC_0 to 0.42 in GC_1. By contrast, the aggregate *DC* (*Default Cascade*) has a significant decrease, from 0.49 to 0.33.

We conclude that for *GC* networks, in which the credit concentration is larger than the debt concentration, an increase in connectivity accompanied by an increase in the concentration of links has the effect of increasing resistance to contagion. Increasing credit concentration in nodes that become major creditors in the system is certainly the factor responsible for the improvement in network resilience against contagion. Very connected creditors have many in-links, so that failure spreads less, only through their few out-links. Moreover, when a neighboring bank of a big creditor defaults, the transmitted loss represents a small fraction of the creditor bank's total exposures because it has many other counterparties. Here we see the positive results of having a major lender that has diversified its risk among many counterparties.

Symmetric networks achieve only a small improvement in resilience when we go from S_0 to S_1. As shown in Table 3, the values of *DI* and *DC* undergo a slight reduction (*DI* varying from 0.46 to 0.43 and *DC* varying from 0.79 to 0.73).

For *GD* networks, the situation is ambiguous: Increased connectivity accompanied by increased link concentration causes a slight reduction in *DI*, from 0.48 to 0.44. At the same time, we see an increase in *Default Cascade*, with *DC* varying from 0.99 to 1.11. For *GD* networks, the increase in link concentration favors the appearance of large debtor banks. These banks have a great potential for contagion because most of their links are directed to the system and thus have a destabilizing role in the network. The fact that *DC* has increased with the increase in connectivity and link concentration is a result of that effect. Even so, the concentration of links also increases the concentration of credit links at creditor banks, which is a stabilizing factor that, with the increase in connectivity, causes a decrease in *DI*.

Increased Connectivity and Link Concentration Similar to Type 0

In type 2, we consider networks in which the average connectivity is raised by increasing β (from 0.25 to 0.75), while we raise δ_{in} and δ_{out} in order to offset the trend of increasing concentration. We maintain the 1:3 ratio between α and γ.

As we have seen in the section "Generating Scale-Free Networks" of the present article, the parameters δ_{in} and δ_{out} represent probabilities distributed equally between nodes, giving every node a chance of being selected in the attachment process. The preferential attachment concentrates links in large connected nodes, while the parameters δ_{in} and δ_{out} can limit this tendency.

With β increased to 0.75, we raise δ_{in} and δ_{out} twenty-five times in order to maintain the Gini coefficient of the links distribution the closest to the value it has in type 0, that is, around 0.45. The best approach we get with $\beta = 0.75$ is a Gini coefficient of 0.47. Table 4 shows the aggregate measures *DI* and *DC* and the values of average connectivity, concentration of links, and partial concentrations (credit links and debt links).

Table 4. Aggregate measures, *DI* and *DC*, < k >, *G*, G_{in} and G_{out}, for network types 0 and 2

	DI	*DC*	< k >	*G*	G_{in}	G_{out}
GC_0	0.433 (±0.001)	0.494 (±0.023)	2.652 (±0.028)	0.456 (±0.008)	0.748 (±0.011)	0.410 (±0.008)
S_0	0.455 (±0.004)	0.792 (±0.024)	2.663 (±0.041)	0.429 (±0.006)	0.578 (±0.015)	0.576 (±0.012)
GD_0	0.480 (±0.004)	0.988 (±0.015)	2.646 (±0.039)	0.457 (±0.006)	0.418 (±0.013)	0.746 (±0.009)
GC_2	0.428 (±0.001)	0.574 (±0.023)	7.813 (±0.200)	0.476 (±0.006)	0.555 (±0.008)	0.465 (±0.007)
S_2	0.429 (±0.001)	0.723 (±0.021)	7.812 (±0.141)	0.471 (±0.008)	0.507 (±0.009)	0.506 (±0.008)
GD_2	0.430 (±0.001)	0.884 (±0.020)	7.817 (±0.139)	0.475 (±0.007)	0.463 (±0.008)	0.554 (±0.007)

When we compare the GC_0 and GC_2 networks, we notice an increase in *Default Cascade, DC*, from 0.49 to 0.57. The default impact index, *DI*, remains stable at 0.43.

Despite our attempt to isolate the connectivity effect by fixing Gini closest to the original value (0.45), we cannot attribute the rise in the *DC* index only to the increased connectivity because while the concentration of links remains close to the original value, there is a variation in the partial concentrations, G_{in} and G_{out}. Indeed, when we change δ_{in} and δ_{out}, we observe an increase in the concentration of debt links in large debtors' nodes (G_{out} varying from 0.41 to 0.46) and a reduction in the concentration of credits (G_{in} from 0.75 to 0.55). These changes contribute to the worsening of the *DC* index.

In the case of symmetric networks, we see a slight improvement in indexes: When we compare the S_0 and S_2 networks, we can see the variation of *DI* from 0.46 to 0.43 and of *DC* from 0.79 to 0.72.

For the *GD* network, an increase in connectivity slightly improves measure *DI*, from 0.48 to 0.43, and also improves the *DC* index, from 0.99 to 0.88. In addition to the increased connectivity, the variation of the partial concentrations, toward a decreased concentration of debts and an increased concentration of credit, is noteworthy.

Increased Connectivity and Lower Link Concentration

The type 3 repeats the experiment of Cont and Moussa (2010) to test increases in connectivity. The type 3 network is built with the same parameter values as type 0. Subsequently, its connectivity is increased by the addition of new links randomly distributed among its nodes. In this way, we have a more connected and less concentrated network: The Gini coefficient goes from 0.45 to 0.24, and the partial Gini coefficients also suffer a reduction. The data are presented in Table 5.

As in types 1 and 2, all three networks (*GC, S*, and *GD*) show a slight improvement in the aggregate impact measure, *DI*, suggesting that the *Default Impact, DI*, decreases with increasing connectivity regardless of whether it is accompanied by an increase or decrease in link concentration. However, the *Default Cascade, DC*, certainly depends on concentrations, as can be seen from the data presented. With increased connectivity and a reduction in the concentration of links (including the partial concentrations), the *GC* network suffers an increase in *Default Cascade, DC*, with the aggregate

Table 5. Aggregate measures, *DI* and *DC*, < k >, *G*, G_{in} and G_{out}, for network types 0 and 3

	DI	*DC*	< k >	*G*	G_{in}	G_{out}
GC_0	0.433 (±0.001)	0.494 (±0.023)	2.652 (±0.028)	0.456 (±0.008)	0.748 (±0.011)	0.410 (±0.008)
S_0	0.455 (±0.004)	0.792 (±0.024)	2.663 (±0.041)	0.429 (±0.006)	0.578 (±0.015)	0.576 (±0.012)
GD_0	0.480 (±0.004)	0.988 (±0.015)	2.646 (±0.039)	0.457 (±0.006)	0.418 (±0.013)	0.746 (±0.009)
GC_3	0.429 (±0.001)	0.678 (±0.020)	7.789 (±0.040)	0.245 (±0.006)	0.378 (±0.010)	0.276 (±0.005)
S_3	0.434 (±0.001)	0.860 (±0.027)	7.800 (±0.041)	0.233 (±0.004)	0.318 (±0.007)	0.317 (±0.005)
GD_3	0.450 (±0.005)	1.007 (±0.017)	7.794 (±0.043)	0.256 (±0.005)	0.277 (±0.005)	0.374 (±0.007)

measure *DC* varying from 0.49 to 0.68. The symmetric network also suffers deterioration in the *DC* index, from 0.79 to 0.85. In turn, the *GD* network has the least change in the index, from 0.99 to 1.01. Again the data suggest that changes in link concentrations are important in determining the *Default Cascade, DC*.

Same Connectivity and Lower Link Concentration

Finally, we test the networks for a decrease in the concentration of links, maintaining the same connectivity. We build type 4 networks by maintaining the same value of β as in the original networks (β = 0.25) and increasing the values of δ_{in} and δ_{out} by a factor of ten.

The indexes of impact, as well as data connectivity and concentration, are shown in Table 6.

For the *GC* and *S* networks, the lowest concentration of links causes a worsening in the indexes of contagion. For these networks, the negative effect of the reduction in concentration of credits is larger than the positive effect of reducing the concentration of debts.

For *GD* networks, the *DI* index shows a slight improvement (from 0.48 to 0.46), whereas the *DC* index worsens (0.99 to 1.01), indicating that in this case the two effects are balanced.

Figure 3 summarizes the results of this section, presenting the *DC* values for the five types of networks analyzed.

Table 6. Aggregate measures, *DI* and *DC*, < *k* >, *G*, G_{in} and G_{out}, for network types 0 and 4

	DI	*DC*	< *k* >	*G*	G_{in}	G_{out}
GC_0	0.433 (±0.001)	0.494 (±0.023)	2.652 (±0.028)	0.456 (±0.008)	0.748 (±0.011)	0.410 (±0.008)
S_0	0.455 (±0.004)	0.792 (±0.024)	2.663 (±0.041)	0.429 (±0.006)	0.578 (±0.015)	0.576 (±0.012)
GD_0	0.480 (±0.004)	0.988 (±0.015)	2.646 (±0.039)	0.457 (±0.006)	0.418 (±0.013)	0.746 (±0.009)
GC_4	0.446 (±0.001)	0.714 (±0.016)	2.644 (±0.048)	0.394 (±0.006)	0.608 (±0.009)	0.385 (±0.011)
S_4	0.459 (±0.001)	0.871 (±0.022)	2.635 (±0.046)	0.388 (±0.007)	0.509 (±0.009)	0.509 (±0.011)
GD_4	0.466 (±0.002)	1.016 (±0.018)	2.661 (±0.036)	0.394 (±0.007)	0.383 (±0.013)	0.607 (±0.010)

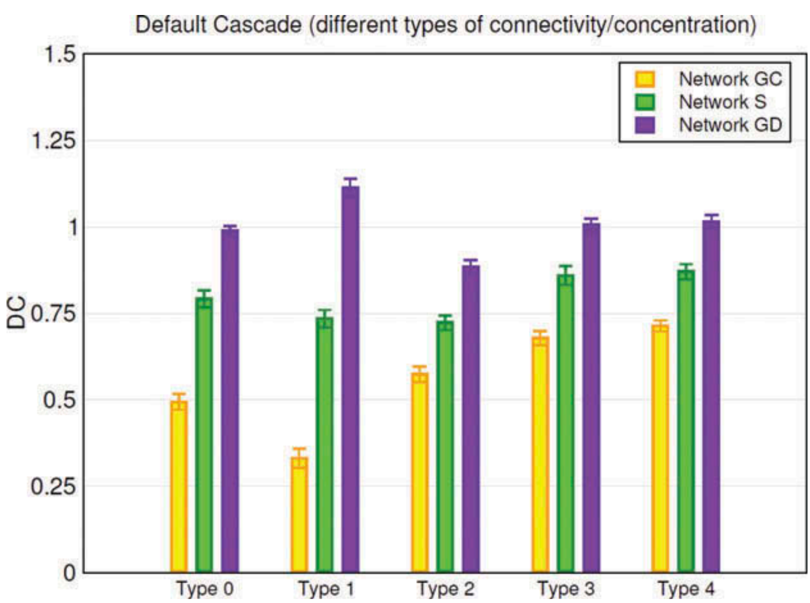

Figure 3. *Default Cascade* (aggregate measure) for the five types of networks analyzed.

The comparisons among these types suggest that for networks constructed with the algorithm of Bollobás et al. (2003) and with exposures positively related to connectivity, the best scenario is one of a more connected network with a high concentration of credits, featuring large creditor nodes, which act as stabilizers of the network. In the comparisons among network types conducted in this work, we do not consider differences among the nodes regarding their probability of default, differences that can change the evaluation of each network type.

Conclusions

In this article, we have analyzed the financial contagion via mutual exposures in the interbank market through simulations of networks whose degree distributions approach power laws.

We have seen that among the measures of systemic importance (*Default Impact* and *Default Cascade, DI* and *DC*), *Default Cascade* (*DC*) is the one that most differentiates the categories of networks analyzed. We also observe that, for all categories, neither the *Default Impact* nor the *Default Cascade* of each node alone reaches a large percentage of the network assets and number of nodes, respectively. This result is consistent with the results of stress tests on empirical networks (Upper 2011).

Comparisons of the different types of networks suggest that, for networks whose distributions are close to power laws and exposure is positively related to connectivity, the best scenario is one with a more connected network with a high concentration of credits, featuring large creditor nodes, which act as stabilizers of the network. These results suggest that the asymmetry observed in distributions of certain real networks is a positive factor, as long as the networks are more concentrated in the distribution of credits (*in*-links).

The results also suggest that the size of the balance sheet is the most important factor in determining the impact on assets resulting from the failure of a node and should not be disregarded or replaced by topological measures that reflect only information on network connectivity. At the same time, the network structure has important consequences for the *Default Cascade*. In some cases, the banks that trigger the largest cascades are not the ones with the bigger balance sheet.

Notes

1. Recall, however, that other interbank networks do not present scale-free characteristics (on the e-MID electronic money market, see, e.g., Fricke and Lux 2015).
2. More recent studies have emphasized core-periphery structures as relevant mechanisms in interbank network formation (Craig and Von Peter 2014; Fricke and Lux 2015). In such models, the idea is that banks organize themselves around a core of intermediaries, giving rise to a hierarchical structure (interbank tiering).
3. In this work, the simulations performed use an initial network, G0, consisting of two nodes, 0 and 1, connected by two directed links, $0 \rightarrow 1$ and $1 \rightarrow 0$.
4. For $\alpha + \gamma = 0.75$, we have $\beta = 0.25$. Since β is the probability of creating a link without addition of a new node, we cannot use a value of β that is too small, otherwise we will have a network with very low average connectivity. However, we would like to have values of α and γ high enough to create asymmetry between the distribution of in-degree and out-degree. The values $\alpha + \gamma = 0.75$ and $\beta = 0.25$ satisfy those requirements.
5. The exponent of a power-law distribution reflects the concentration of the distribution: A smaller absolute value of the exponent corresponds to a more concentrated distribution. Therefore, differences between exponents X_{IN} and X_{OUT} represent differences between the concentrations of the in- and out-degree distributions.
6. The concentration of assets in real networks is also quite high, as reported in the literature. For example, Elsinger, Lehar, and Summer (2006) report a Gini coefficient of 0.88 for the Austrian network in 2002, and Ennis (2001) reports a Gini coefficient of 0.90 for the United States in 2000.
7. The equation for DI_i excludes from its computation the value of initial impact (NBA_i), representing only the losses due to contagion.

References

Allen, F., and D. Gale. 2000. Financial contagion. *Journal of Political Economy* 108 (1):1–33. doi:10.1086/262109.

Arinaminpathy, N., S. Kapadia, and R. May. 2012. Size and complexity in model financial systems. *Proceedings of the National Academy of Sciences* 109 (45):18338–43. doi:10.1073/pnas.1213767109.

Barabasi, A.-L., and R. Albert. 1999. Emergence of scaling in random networks. *Science* 286 (5439):509–12. doi:10.1126/science.286.5439.509.

Battiston, S., D. D. Gatti, M. Gallegati, B. Greenwald, and J. E. Stiglitz. 2012. Liaisons dangereuses: Increasing connectivity, risk sharing, and systemic risk. *Journal of Economic Dynamics and Control* 36 (8):1121–41. doi:10.1016/j.jedc.2012.04.001.

Bollobás, B., C. Borgs, C. Chayes, J. T. Chayes, and O. Riordan. 2003. *Directed scale-free graphs*. In Proceedings of the 14th ACM-SIAM Symposium on Discrete Algorithms, pp. 132–39, Baltimore, MD, USA, November 2003, ACM/SIAM.

Boss, M., H. Elsinger, M. Summer, and S. Thurner. 2004. Network topology of the interbank market. *Quantitative Finance* 4 (6):677–84.

Clauset, A., C. R. Shalizi, Newman, and M. E. J. Newman. 2009. Power-law distributions in empirical data. *SIAM Review* 51 (4):661–703. doi:10.1137/070710111.

Cont, R., and A. Moussa. 2010. Too interconnected to fail: Contagion and systemic risk in financial networks. Financial engineering report, Columbia University, New York, NY.

Cont, R., A. Moussa, E. B. Santos, and Santos. 2010. Network Structure and Systemic Risk in Banking Systems. Available at SSRN: http://ssrn.com/abstract=1733528 or http://dx.doi.org/10.2139/ssrn.1733528.

Craig, B., and G. von Peter. 2014. Interbank tiering and money center banks. *Journal of Financial Intermediation* 23 (3):322–47. doi:10.1016/j.jfi.2014.02.003.

Eisenberg, L., and T. Noe. 2001. Systemic risk in financial systems. *Management Science* 47 (2):236–49. doi:10.1287/mnsc.47.2.236.9835.

Elsinger, H., A. Lehar, and M. Summer. 2006. Risk assessment for banking systems. *Management Science* 52 (9):1301–14. doi:10.1287/mnsc.1060.0531.

Ennis, H. M. 2001. On the size distribution of banks. *Federal Reserve Bank of Richmond Economic Quarterly* 87 (4):1–25.

Freixas, X., B. Parigi, and J.-C. Rochet. 2000. Systemic risk, interbank relations and liquidity provision by the central bank. *Journal of Money, Credit and Banking* 32:611–38. doi:10.2307/2601198.

Fricke, D., and T. Lux. 2015. Core-periphery structure in the overnight money market: Evidence from the e-MID trading platform. *Computational Economics* 45 (3):359–95.

IMF (International Monetary Fund). 2013. Financial Soundness Indicators. http://fsi.imf.org (accessed September 15, 2015).

Inaoka, H., T. Ninomiya, K. Taniguchi, T. Shimizu, and H. Takayasu. 2004. Fractal network derived from banking transaction: An analysis of network structures formed by fifinancial institutions. Bank of Japan working papers 04E-04, Bank of Japan, Tokyo, Japan.

Ladley, D. 2013. Contagion and risk-sharing on the inter-bank market. *Journal of Economic Dynamics and Control* 37 (7):1384–400. doi:10.1016/j.jedc.2013.03.009.

Mistrulli, P. E. 2011. Assessing financial contagion in the interbank market: Maximum entropy versus observed interbank lending patterns. *Journal of Banking & Finance* 35 (5):1114–27. doi:10.1016/j.jbankfin.2010.09.018.

Montagna, M., and T. Lux. 2014. Contagion risk in the interbank market: A probabilistic approach to cope with incomplete structural information. FinMaP Working Paper 8, Kiel University, Kiel, Germany.

Nier, E., J. Yang, T. Yorulmazer, and A. Alentorn. 2007. Network models and financial stability. *Journal of Economic Dynamics and Control* 31 (6):2033–60. doi:10.1016/j.jedc.2007.01.014.

Soramäki, K., M. L. Bech, J. B. Arnold, R. J. Glass, and W. Beyeler. 2007. The topology of interbank payment flows. *Physica A: Statistical Mechanics and Its Applications* 379 (1):317–33. doi:10.1016/j.physa.2006.11.093.

Upper, C. 2011. Simulation methods to assess the danger of contagion in interbank markets. *Journal of Financial Stability* 7 (3):111–25. doi:10.1016/j.jfs.2010.12.001.